AIAA JOURNAL
Vol. 40, No. 2, February 2002

Buckling of Composite Plates with Local Damage and Thermal Residual Stresses

Sérgio Frascino Müller de Almeida*
Instituto Tecnológico de Aeronáutica 12228-900 São José dos Campos, Brazil
and
Jorn S. Hansen†
University of Toronto, Downsview, Ontario M3H 5T6, Canada

The interactive effect of manufacturing induced thermal residual stresses and structural damage on the buckling load of stringer stiffened composite plates is investigated. The study is motivated from the consideration that the thermal effects have been tailored to enhance the plate buckling loads. Thus, it is crucial to understand the influence of and sensitivity to structural damage. Damage is considered either in the form of localized degradation of material properties or as delamination between the plate and stiffeners. Both damage types are characterized in terms of type, amount, shape, and size. It is shown that thermal residual effects may increase or decrease buckling-load damage sensitivity and that the sensitivity is damage location dependent. For all cases, the numerical analyses demonstrate that plates with tailored thermal residual effects have good damage tolerance and that this is a direct result of a redistribution of residual stresses. Thermal residual effects improve the buckling load for both damaged and undamaged plates. A particularly interesting result occurs when a plate with localized damage at its center is considered; the buckling load can actually increase with the introduction of damage when thermal effects are included in the analysis.

Introduction

EFFECTIVE design of composite structure requires extensive use of concurrent engineering concepts as design, manufacturing process, and material selection are intimately intertwined. A good design should account not only for performance requirements, but also for manufacturing parameters, which may significantly affect structural performance. That is, the manufacturing process must be considered in the composite structural design not only to avoid deleterious effects, but also to capitalize on advantageous effects.

Manufacturing induced thermal residual stresses are always present in laminated polymeric composites. These stresses manifest themselves at three different levels related to the micromechanical, lamina, and laminate length scales. The microscopic level stresses result from the difference in the thermal expansion coefficient of the fiber and matrix and chemical shrinkage (for thermosets) or crystallization (for thermoplastics) of the matrix. These stresses depend on processing parameters and affect the strength of the material.[1,2] However, they do not appear in macroscopic elastic analyses in which the through the thickness stress resultants are zero.

At a macroscopic level, the manufacturing induced stresses occur because of the anisotropy of the thermal expansion coefficient of a lamina. Typically, the thermal expansion coefficient is much smaller in the fiber direction than in the transverse direction. Therefore, when a laminate is formed from laminas with different fiber orientations, thermal stresses arise as the material cools from the processing temperature to the operating temperature. These stresses appear at the macroscopic level and affect the laminate strength.[3] Note that laminate thermal residual stresses affect elastic structural response only when the stress resultants are nonzero. Therefore, although thermal residual stresses are always present at a lamina level, they are not necessarily important at the laminate level. This situation occurs, for example, in a uniform, unconstrained symmetric laminate where the thermal residual stresses have no direct effect on the plate geometry or the elastic response. Therefore, for this situation, thermal stresses affect laminate strength but not the laminate stiffness.

Thermal stress resultants are nonzero for constrained plates, nonsymmetric laminates, and spatially heterogeneous structures such as plates with stiffeners. The latter represent an important case in terms of practical engineering applications including the civil, transport, and aerospace sectors. Typically, composite stiffeners are constructed with the lamina fiber directions primarily oriented along the length of the stiffener, and, therefore, the stiffeners have a thermal expansion coefficient smaller than that of the plate proper. In this situation, the stiffened plate is spatially heterogeneous and in general nonzero thermal stress resultants are present because of the mismatch between the thermal expansion coefficients of the stiffener and the plate; this is true even for unconstrained symmetric configurations. As a result, a reinforced plate may contain large tensile thermal residual stresses while the stiffeners are in compression. The existence of these thermal residual-stress resultants affects the bending stiffness of the plate because of stress stiffening effects.

Almeida and Hansen[4] introduced the idea of tailoring these manufacturing induced residual stress resultants to enhance the structural response of composite structures. They demonstrated numerically that the buckling load[4] and natural frequencies[5] of composite plates with stiffeners could be very substantially affected by the thermal stress resultants. These calculations have been verified by Sarath Babu and Kant[6] and Foldager.[7]

Note that thermal stress resultants are present either when the stiffeners and plate are cocured or when secondary bonding is used. In the latter situation, the plate is free of thermal residual stresses only at the adhesive cure temperature. The magnitudes of the thermal stresses depend directly on the relative magnitude of the cure or secondary bonding temperature; however, either manufacturing process will affect the structural response.

Another example of using thermal residual stresses to enhance structural response involves the design of composite patches for repair of aircraft parts. The patch design should be such that compressive thermal residual stresses resulting from the different coefficient of thermal expansion of the repaired structure and patch inhibits damage propagation.[8]

Received 30 May 2000; revision received 15 May 2001; accepted for publication 5 July 2001.

*Professor, Department of Mechanical Engineering; frascino@mec.ita.cta.br.

†Professor, Institute for Aerospace Studies, 4925 Dufferin Street; hansen@utias.utoronto.ca.

The magnitude of thermal residual-stress resultants depends on a number of factors: plate geometry and construction, physical properties of the materials used, cure (or consolidation) temperature, etc. Of course, the effect of the thermal stress resultants on the structural behavior also depends on those variables. Therefore, the process of tailoring the thermal residual-stress resultants to enhance a particular characteristic of the structure requires a judicious choice of the design variables such that a favorable residual-stress distribution is present in the structure.

The number of variables involved in the determination of the magnitude of the thermal residual-stress resultants and their effect on the structural performance may be quite large. Moreover, the problem is complex, and therefore, it is usually not possible to predict whether a configuration is favorable without resorting to numerical analysis. Thus, optimization procedures must be used to determine the design that minimizes the structural weight subject to a given set of design constraints.[9] Ignoring thermal residual-stress resultants in an optimization procedure may result in designs where the effect of thermal residual-stress resultants is quite deleterious. For, even if thermal residual effects are ignored in analysis and design, these effects are definitely present in actual composite structure. Furthermore, numerical results by Foldager[7] show that the buckling load of optimal stiffened cylindrical shells may decrease by a factor of five when thermal stresses corresponding to a difference of 100°C between the cure temperature and the operating temperature are included in the analysis. That is, ignoring manufacturing induced thermal effects may grossly overestimate the structural capacity of an optimal design.

Damage tolerance is an important consideration in the design of composite structure. This is particularly true in the presence of thermal residual-stress resultants as inservice damage may cause a redistribution of residual stresses. This redistribution may lead to a dramatic deterioration of the structural performance, and therefore, thermal residual-stress effects must be included when assessing damage tolerance.

Previous work[4] has demonstrated that stiffened composite plates can be tailored such that thermal residual stresses may significantly enhance the buckling load and, therefore, must be taken into account in the analysis. The present work analyzes the interaction between structural damage and thermal residual stresses addressing the question whether the presence of structural damage eliminates the benefits introduced by thermal residual stresses. In the analyses, damage is characterized in terms of type, amount, shape, and size. Two types of damage are considered: 1) localized damage, modeled as an effective stiffness reduction, and 2) delamination, modeled by changes in the finite element model. The numerical results show that, for the cases studied, plates with thermal residual stresses have good damage tolerance. That is, the stress redistribution resulting from damage is quite favorable, and therefore, the superior performance is retained compared to plates in which thermal residual effects are ignored.

Structural Analysis

The analysis used in the present work is based on the approach of Almeida and Hansen.[4] A composite laminated plate subjected to in-plane compressive loads is considered. Each lamina is assumed to be orthotropic, homogeneous, and linear elastic. Also, stiffened plates are considered, and therefore, thermal residual-stress resultants due to the cure or consolidation process are present. The problem under consideration is divided into three subproblems: the thermal, prebuckling, and buckling problems. Calculations are based on laminated Reissner–Mindlin plate theory. The analysis is quite general, with the only restriction being that the laminate is symmetric, and therefore, no linear membrane–bending coupling exists. This restriction is imposed because the cure/consolidation of a nonsymmetric laminate will cause thermally induced out-of-plane deformations, and these deformations lead to totally different analysis requirements (such a plate would no longer be a plate but would be a shell). The basic hypotheses assumed for the solution of each of the three subproblems described earlier and the finite element procedure used to solve them are discussed in the following.

Thermal Problem

First, the thermally induced effects due to the cure/consolidation must be evaluated. This aspect of the problem is solved in a general form with the only restrictions being that the laminate is symmetric and that the analysis is linear. In this calculation, the plate–stiffener assembly is assumed to be completely unconstrained; thus, residual stress resultants arise only from thermal coefficient of expansion mismatches either through the thickness of the laminate or due to spatial variations in the thermal coefficient of expansion.

Note that the material properties are in general functions of temperature, and at elevated temperatures viscoelastic/relaxation effects are to be expected. These aspects, however, are not included in the present formulation. Therefore, the computed thermal stresses based on room temperature material properties should be interpreted as corresponding to an equivalent lower cure temperature; the value of the temperature difference ΔT should be corrected accordingly.

Prebuckling Problem

The second step is the calculation of the prebuckling state of the plate–stiffener assembly. When boundary conditions are applied, it is assumed that no mechanically induced stresses are imposed on the system. The loading state in the prebuckling problem is assumed to result from the application of a uniform displacement applied on the plate boundary of interest. This calculation is assumed linear with no membrane–bending coupling; the results of this calculation are nonuniform displacement fields with associated stress and strain fields. Because of the nonuniformity of the prebuckling state, the buckling problem does not exhibit the inherent simplicity of classical buckling problems in which the buckling load is directly related to uniform stress resultants.

Buckling Problem

The third and final step is the buckling calculation. Full nonlinear strain–displacement relations are assumed for this analysis. This problem is solved by representing the solution as a sum of the combined thermal/prebuckling subproblems and the buckling state. Individually these states are assumed to be linear while the nonlinearity in the problem contributes to the interaction between the thermal/prebuckling and the buckling problems. The linear buckling problem is an eigenvalue problem that yields buckling loads and associated buckling modes. Note that the buckling load is not obtained directly; rather it is the total force required to produce the critical displacement at the loaded plate edge. Such a model is representative of the manner in which plates are loaded in actual experimental configurations.

Finite Element Formulation

A finite element formulation was developed to solve the problem described in the preceding section. A 16-node bicubic isoparametric quadrilateral element using Lagrange interpolation functions was implemented in a FORTRAN code by Almeida and Hansen.[4] The element has 5 degrees of freedom per node with a total of 80 degrees of freedom per element. The element stiffness matrix and element geometric stiffness matrix are computed numerically using Gauss quadrature with 4×4 integration points. A shear correction factor of $\frac{5}{6}$ is used for all laminates.

The eigenvalue problem for the linear buckling analysis of the plate is

$$\left\{[K] + \left[K_G^R\right] - \lambda\left[K_G^0\right]\right\}\{\delta\} = \{0\} \tag{1}$$

The matrices $[K]$, $[K_G^R]$, and $[K_G^0]$ are, respectively, the global stiffness matrix, the global geometric stiffness matrix due to thermal residual-stress resultants, and the global geometric stiffness matrix due to prebuckling stress resultants computed for a unit positive displacement. Variable λ characterizes the magnitude of the prebuckling displacement and yields the buckling displacement and in turn the buckling load.

Damage Modeling

There are many possible failure mechanisms in laminated composites, and this makes modeling damage quite complex. Low-velocity impact causes primarily delamination and matrix

cracking,[10] whereas high-velocity impact may cause fiber fracture as well. Damage depends on the problem geometry, laminate ply orientation, and thickness, as well as the mass and velocity of the impactor; impact damage may cause a significant reduction in the strength and stiffness of the structure.

Two types of damage are considered in this work, namely, localized damage over a circular area and delamination between the stiffener and plate. Such damage affects the distribution of thermal residual stresses and in turn the plate buckling load.

Localized Damage

Here, damage is modeled as an effective reduction in the value of the local elastic moduli. This approach is often used to assess damage effects on the elastic behavior of structures[11] and is suitable for the purposes of the present work. The study aims to provide a conservative assessment of plate damage tolerance in the presence of thermal residual-stress resultants when a buckling load requirement is prescribed.

Local damage is characterized by shape, location, and degree. The damage region is assumed to be circular with radius r. Damage regions are considered at the center, side, or corner of the plate; these configurations are shown in Fig. 1. Note that, when the damage is located either at the side or corner of the plate, then the degraded area includes portions of both the stiffener and skin. Finally, the degree of damage is controlled by a parameter α that multiplies the elastic properties of the material within the damage region. This parameter varies from 0 to 1: $\alpha = 1$ corresponds to undamaged material; $\alpha = 0$ represents complete material destruction and is equivalent to a hole of radius r in the laminate. Implementing the limiting case of $\alpha = 0$ using the original finite element mesh results in numerical difficulties because certain finite element nodes have no associated stiffness; thus, to model complete material destruction $\alpha = 0.01$ was used. The accuracy of this approximation is discussed later in the work.

Stiffener Delamination

The second type of damage considered is delamination between the plate and stiffener. Symmetric delaminations spanning length $2L$ on both sides of the plate and along the entire width of the stiffener are considered; this is shown in Fig. 2. This representation of the damage is expected to be conservative and is used to maintain laminate symmetry and thereby avoid membrane–bending coupling as discussed earlier. If the delamination is not symmetric, the linear buckling problem will not yield realistic results.

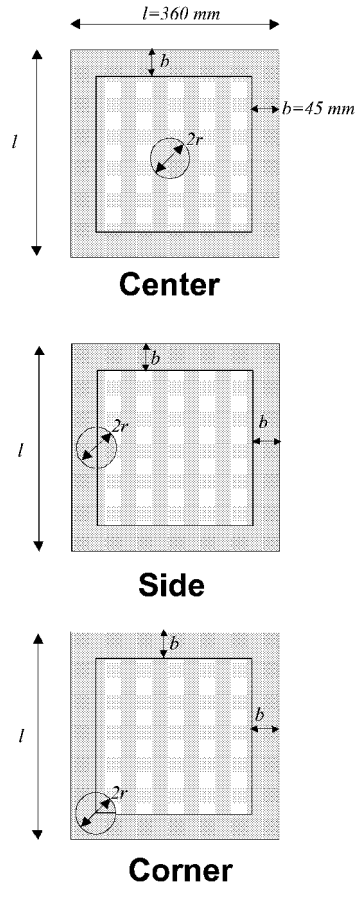

Fig. 1 Damage locations considered.

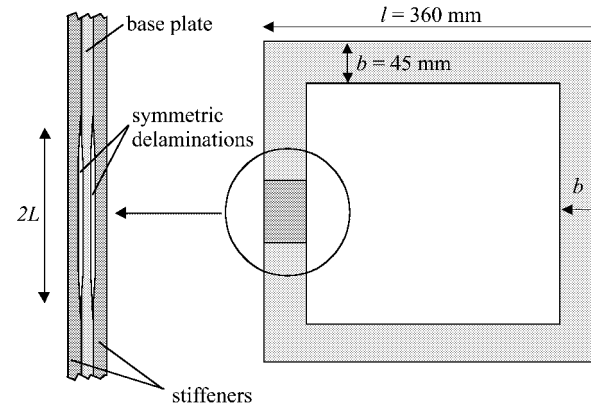

Fig. 2 Geometry of stiffener delamination.

Note that local buckling of the stiffener over the delaminated region may cause propagation of the delamination and a reduction of plate stiffness; this problem is not considered here. The current model includes the effects of stiffener delamination on plate stiffness by appropriate changes in the finite element model; this will be described in the following section. The plate buckling load is affected by the combined effects of the stiffness change and the redistribution of the thermal residual-stress resultants.

Numerical Results and Discussion

The effect of damage on the buckling load of composite plates will be analyzed for one of the geometrical configurations used by Almeida and Hansen.[4] The chosen configuration corresponds to the case for which the effect of the thermal residual-stress resultants is the most significant among those studied. Therefore, it represents a case where damage-induced residual-stress relief may cause a significant degradation of the structural performance. Also, the plate is easy to manufacture and of practical significance.

The plate used for all analyses is a square $[90/0]_s$ laminate of dimensions $l \times l$ with stiffeners of width b symmetrically bonded to the top and bottom surfaces. The stiffeners are composed of four unidirectional plies placed around the perimeter of the plate. Figure 3 shows the geometry and the resulting lamination sequence for each region of the plate. Ply drops are used at the corners (laminate L3) to maintain the stiffeners thickness constant. The plate is simply supported on all edges and is loaded in the y direction; the lamination angle for each ply is measured with respect to the y axis. The plate length and stiffener width are $l = 360$ mm and $b = 45$ mm, respectively, for all analyses. All buckling loads are normalized with respect to the buckling load of the undamaged configuration in the absence of thermal effects.

The plate shown in Fig. 3 is analyzed using the formulation described earlier including the two types of damage. The plate is assumed to be manufactured using graphite/epoxy cured at 180°C and tested at 30°C. Thermal stress fields result from the difference between the processing and working temperature, and this difference is designated as ΔT; for example, $\Delta T = -150$°C corresponds to a typical room temperature operating situation, whereas $\Delta T = 0$°C corresponds to a model where thermal effects are neglected. The physical properties for graphite/epoxy are assumed the same as those used by Almeida and Hansen,[4,5] and are given in Table 1.

Localized Damage

The finite element model is based on a regular 8×8 mesh except in the damage region where local refinement is necessary. The finite element mesh is refined locally to model the circular damage. Figure 4 shows the finite element mesh used; 20 quadrilateral elements replace the appropriate 4 elements of the undamaged plate. The stiffness of the elements within the shaded area are multiplied

Table 1 Lamina properties used for T300/5208 graphite/epoxy

Property	Value
Longitudinal modulus of elasticity E_1	154,500 MPa
Transverse modulus of elasticity E_2	11,130 MPa
In-plane Poisson's ratio ν_{12}	0.304
In-plane shear modulus G_{12}	6,980 MPa
Transverse shear modulus G_{13}	6,980 MPa
Transverse shear modulus G_{23}	3,360 MPa
Longitudinal thermal expansion coefficient α_1	$-0.17e{-}06^{\circ}\mathrm{C}^{-1}$
Transverse thermal expansion coefficient α_2	$23.1e{-}06^{\circ}\mathrm{C}^{-1}$
Ply thickness t	0.15 mm

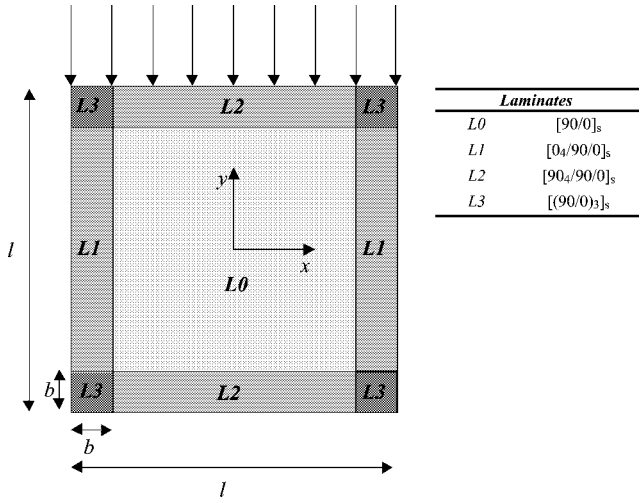

Laminates	
L0	$[90/0]_s$
L1	$[0_4/90/0]_s$
L2	$[90_4/90/0]_s$
L3	$[(90/0)_3]_s$

Fig. 3 Plate geometry and the lamination sequence for each region.

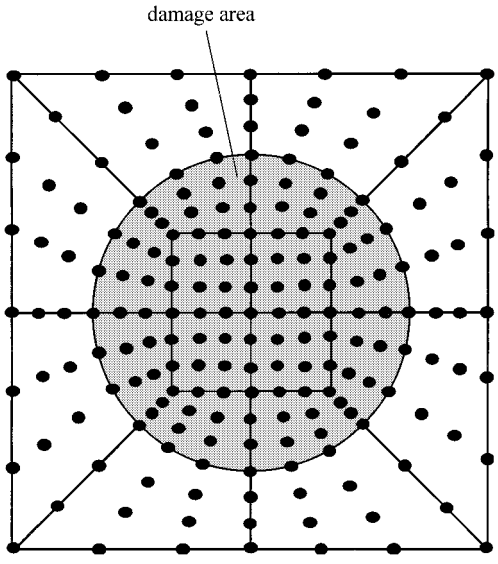

Fig. 4 Finite element mesh used to model the localized damage.

by α. Unlike the problems studied previously,[4,5] the present problem geometry is not symmetric due to the presence of damage; the mesh used yields accuracy equivalent to that used earlier.

As already noted, numerical difficulties arise as the value of α approaches 0. A convergence study was performed to assess the accuracy of the model for this situation. Table 2 lists the buckling load of a plate with a 36-mm-radius damage at its center for $\Delta T = 0$ and -150°C. The buckling loads were calculated for a sequence of values as α approaches zero. An analysis with $\alpha = 10^{-10}$ was performed to obtain reference values for the total destruction of the material. In this case, all degrees of freedom corresponding to nodes within the damaged area were eliminated to avoid numerical difficulties. The results indicate that the model using α approaching zero

Table 2 Convergence study for value of α approaching zero: Analysis of plate with 36-mm damage at its center

α	P_{cr} for $\Delta T = -150^{\circ}$C, N	P_{cr} for $\Delta T = 0^{\circ}$C, N
0.050	1903.1	456.0
0.030	1928.3	461.5
0.020	1942.9	464.9
0.010	1958.9	468.6
0.005	1967.5	470.7
0.003	1971.2	471.5
0.002	1973.0	472.0
0.001	1974.8	472.3
10^{-10}	1976.7	472.7

correctly converges to the reference values within the studied range. The analyses with $\alpha = 0.01$ produce estimates of the plate buckling load with a hole to within an accuracy of 1% of the reference values. Therefore, all analyses in the present work were performed for $0.01 \leq \alpha \leq 1$.

Figures 5a–5c present buckling load variation with respect to α for damage located at the center, side, and corner of the plate, respectively. Note that the buckling load is normalized with respect to the buckling load of the undamaged plate for $\Delta T = 0^{\circ}$C and α varies from 1 to 0.01; that is, damage increases from left to right.

Figure 5a shows that there is little influence on the buckling load when damage is located at the plate center and thermal stresses are ignored. However, when thermal residual stresses are included in the formulation, the buckling load actually increases as damage increases. A gain of approximately 10% is observed for damage with a 36 mm radius. This unexpected result is explained by the redistribution of the thermal residual-stress resultants due to the existence of damage. Figures 6a and 6b compare the distribution of the principal values of thermal residual-stress resultants for $\alpha = 1$ and 0.01. In Fig. 6 the arrows indicate the principal stress direction and magnitude; arrows directed upward or to the right correspond to tension, whereas downward and left-pointing arrows are associated with compressive thermal residual-stress resultants. Thus, as can be seen in Fig. 6a, the stiffeners are in compression, whereas the plate is in tension with the largest tensile stresses occurring adjacent to the stiffeners. The presence of damage causes a redistribution of thermal stress resultants. The stress resultants at the center of the plate are most affected with the radial components vanishing at the edge of the hole. However, stress resultants tangential to the hole and stresses near the stiffener are still present and cause a favorable effect increasing the buckling load. This is similar to the result observed by Teng[11] for circular plates where buckling loads increased as damage increased.

Figures 5b and 5c demonstrate that the side and corner of the plate are unfavorable locations for damage because the buckling load reduces with increasing damage. However, note that damage at the plate edge causes similar relative reductions in buckling load both when thermal residual-stress resultants are considered or omitted. A damage diameter equal to 20% of the plate length ($r = 36$ mm) causes a reduction of about 17% in the buckling load even for $\alpha = 0.01$. Therefore, it can be said that the plate with thermal residual-stress resultants is quite tolerant of damage at this location. If thermal effects are neglected, there is a decrease of 27% in the buckling load for $\alpha = 0.01$.

Among the damage locations considered in this work, corner damage is the most unfavorable for plates with thermal residual stress. The decrease in buckling load is quite moderate when thermal residual-stress resultants are not accounted for (less than 20%) but may be significant when they are included in the formulation. However, note that even though the buckling load is reduced by a factor of approximately 2 for damage with radius 36 mm and $\alpha = 0.01$, the plate with thermal residual-stress effects included still yields a buckling load that is significantly higher (a factor of 2.1) than the plate in which these effects are ignored.

In summary, note that the calculation including thermal residual stresses yields higher buckling load for all cases analyzed in this

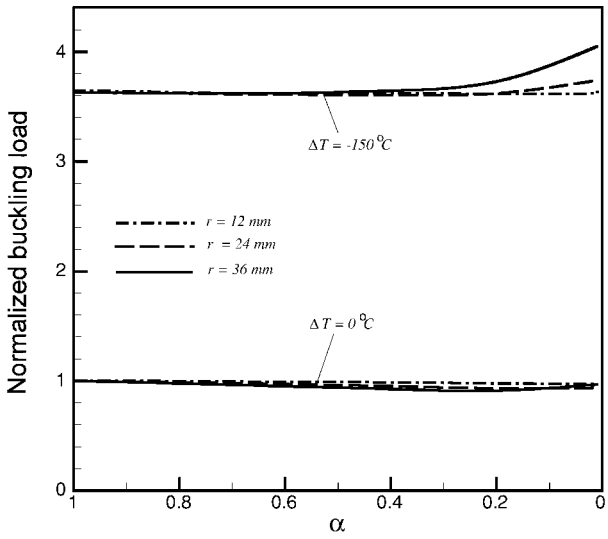

Fig. 5a Normalized buckling load as a function of parameter α for damage at the center of the plate.

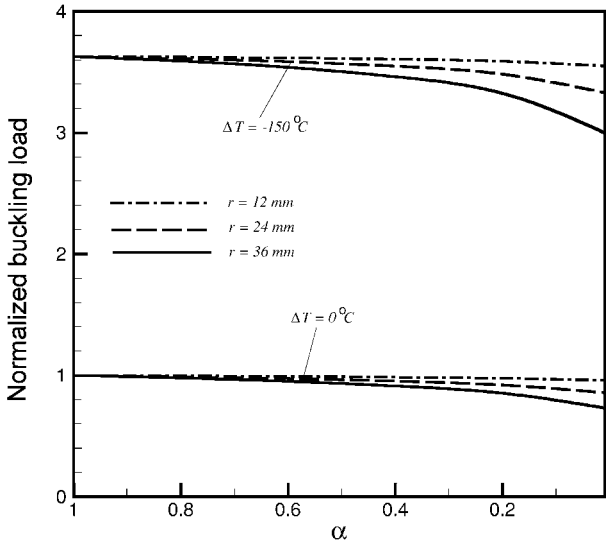

Fig. 5b Normalized buckling load as a function of parameter α for damage at the side of the plate.

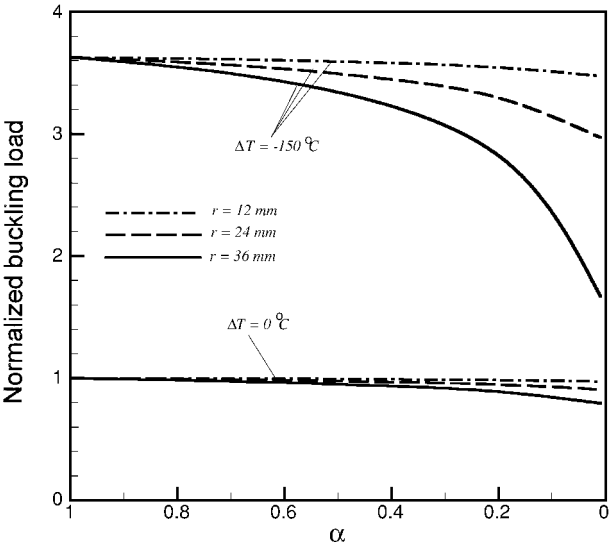

Fig. 5c Normalized buckling load as a function of parameter α for damage at the corner of the plate.

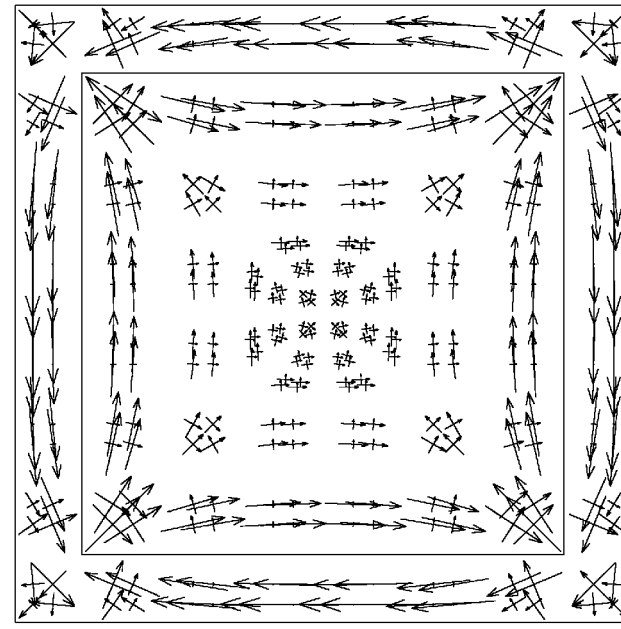

Fig. 6a Distribution of thermal stress resultants for $\alpha = 1$.

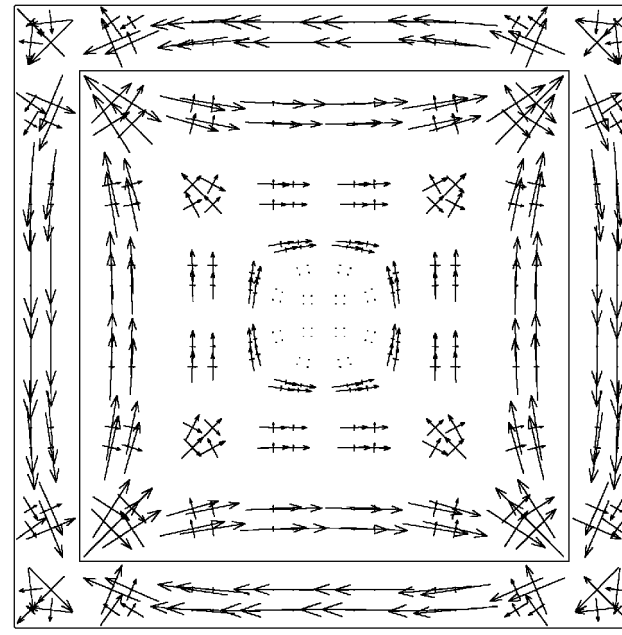

Fig. 6b Distribution of thermal stress resultants for $\alpha = 0.01$.

section. Thus, it may be concluded that the structural effectiveness of these plates may be underestimated if thermal processing effects are ignored. In addition, the results demonstrate that such plates can sustain significant damage without a serious reduction in buckling load.

Stiffener Delamination

A symmetric stiffener delamination of length $2L$ is now considered (Fig. 2). Again, the finite element model is based on a regular 8×8 mesh except in the delamination region where proper modeling of the stiffeners is necessary. Two representations of the delamination are analyzed. In the first, the delaminated section of the stiffener and base plate under the delaminated stiffener are both modeled using two bicubic elements that share nodes at the ends of the delamination but with no other interaction; contact problems and delamination growth are not considered. In the second configuration, the stiffeners are assumed to give no structural contribution after delamination and are, thus, removed from the finite element model over the delaminated area. Figure 7 shows the effect of the

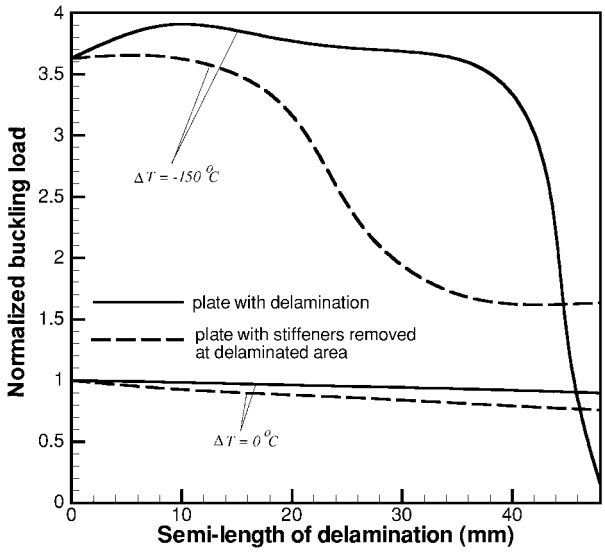

Fig. 7 Normalized buckling load as a function of the semilength of the delamination.

delamination semilength on the normalized buckling load of the plate for the two representations.

Note that the geometry assumed for the delamination is very conservative and unlikely to occur in a practical application. The choice of this configuration is primarily dictated by the analysis requirements discussed earlier.

The numerical results show that delamination has little effect on the buckling load when thermal residual resultants are ignored. When the stiffeners and thermal residual-stress resultants are included in the model, the buckling load increases for small delamination lengths because of a favorable redistribution of the thermal stresses. However, for the semilength approximately equal to 36 mm, local buckling of the stiffeners over the delaminated area occurs, and the buckling load decreases dramatically for larger delaminations. For a sufficiently large delamination, the stiffeners buckle over the delaminated area from thermal effects alone even in the absence of mechanical loads.

The representation without stiffeners over the delaminated area is a lower bound for the buckling load of the plate assuming that no delamination growth occurs. In this case, the buckling load decreases sharply for semilength $L > 20$ mm. However, within the range analyzed, the buckling load is always higher when thermal effects are included.

An important design consideration is delamination growth. Even though local buckling of the stiffener may be acceptable in terms of design, this condition may cause delamination growth and possibly a catastrophic failure. Therefore, the maximum admissible delamination should be such that local buckling of the stiffeners is avoided ($L < 36$ mm). This conservative estimate shows that the plate with tailored thermal stress resultants can sustain a relatively large stiffener delamination without significant loss in the buckling load.

Conclusions

The effect of damage on the buckling load of a stiffener-reinforced composite plate with tailored processing induced thermal residual stresses is assessed. Two types of damage are considered and characterized in terms of type, degree, shape, and size. For all configurations considered, the results demonstrate that plates in which thermal residual stresses are included in the analysis have good damage tolerance as compared to the case when the thermal effects are ignored. This results from the redistribution of the thermal residual stresses due to the damage. Thus, it may be concluded that a beneficial prebuckling residual-stress state will be totally ignored if thermal residual-stress effects have been omitted from the analysis.

It is shown that buckling load damage sensitivity depends on damage type and location. The presence of thermal effects may increase or decrease the sensitivity to damage depending on damage location. A particularly interesting result is that the buckling load of a plate with localized damage at the center can actually increase with damage when thermal effects are included. For other damage locations, the stress redistribution is not favorable, and thermal effects result in a greater sensitivity to damage. However, for all cases analyzed, higher buckling load are obtained when thermal residual stresses are included in the analysis. Thus, it is concluded that plates with tailored thermal stress resultants can sustain substantial damage without significant loss in the buckling load.

Acknowledgments

The first author acknowledges financial support received from the State of São Paulo Research Foundation, Grant 99/09580-0, and the Brazilian National Research Council, Grant 300219/90-3. The second author acknowledges financial support received from Natural Sciences and Engineering Research Council of Canada Grant 3663.

References

[1] White, S. R., and Hahn, H. T., "Process Modeling of Composite Materials: Residual Stress Development During Cure. Part I. Model Formulation," *Journal of Composite Materials*, Vol. 26, No. 16, 1992, pp. 2402–2422.

[2] Unger, W. J., and Hansen, J. S., "The Effect of Thermal Processing on Residual Strain Development in Unidirectional Graphite Fibre Reinforced PEEK Laminates," *Journal of Composite Materials*, Vol. 27, No. 1, 1993, pp. 59–82.

[3] Jones, R. M., *Mechanics of Composite Materials*, McGraw–Hill, New York, 1975.

[4] Almeida, S. F. M., and Hansen, J. S., "Enhanced Elastic Buckling Loads of Composite Plates with Tailored Thermal Residual-Stresses," *Journal of Applied Mechanics*, Vol. 64, No. 4, 1997, pp. 772–780.

[5] Almeida, S. F. M., and Hansen, J. S., "Natural Frequencies of Composite Plates with Tailored Thermal Residual-Stresses," *International Journal of Solids and Structures*, Vol. 36, No. 23, 1999, pp. 3517–3539.

[6] Sarath Babu, C., and Kant, T., "Letter to the Editor: Enhanced Elastic Buckling Loads of Composite Plates with Tailored Thermal Residual-Stresses," *Journal of Applied Mechanics*, Vol. 65, No. 4, 1998, pp. 1070, 1071.

[7] Foldager, J. P., "Design of Composite Structures," Ph.D. Dissertation, Inst. of Mechanical Engineering, Special Rept. 39, Aalborg Univ., Aalborg, Denmark, 1999.

[8] Renaud, G., and Hansen, J. S., "Thermal Model for Cracked Structures with Composite Patches," *AIAA Journal*, Vol. 36, No. 12, 1998, pp. 2229–2235.

[9] Faria, A. R., and Hansen, J. S., "Optimal Buckling Loads of Nonuniform Composite Plates with Thermal Residual Stresses," *Journal of Applied Mechanics*, Vol. 66, No. 2, 1999, pp. 388–395.

[10] Choi, H. Y., and Chang, F. K., "A Model for Predicting Damage in Graphite/Epoxy Laminated Composites Resulting from Low-Velocity Point Impact," *Journal of Composite Materials*, Vol. 26, No. 14, 1992, pp. 2134–2169.

[11] Teng, J. G., "Why Local Damage Increases the Buckling Load of Circular Plates," *Thin Walled Structures*, Vol. 34, No. 2, 1999, pp. 147–161.

A. M. Waas
Associate Editor